

Mapping Dark Atomic and Molecular Gas in the Galaxy

S. J. Gibson¹, A. C. Bell^{1,2}, J. H. Newton^{1,3}, W. S. Howard⁴, C. S. Jolly^{1,5}, M. E. Spraggs^{1,5}, J. M. Hughes^{1,5}, C. M. Brunt⁶, A. R. Taylor⁷,
A. Noriega-Crespo⁸, W. T. Reach⁸, S. Carey⁸, B-C. Koo⁹, G. Park⁹, T. Dame¹⁰, IGPS Consortium, I-GALFA Consortium

¹Western Kentucky U., ²U. Tokyo, ³McMaster U., ⁴Union U., ⁵C. M. Gatton Acad., ⁶Exeter U., ⁷U. Calgary, ⁸IPAC, ⁹Seoul Nat. U., ¹⁰Harvard-CfA

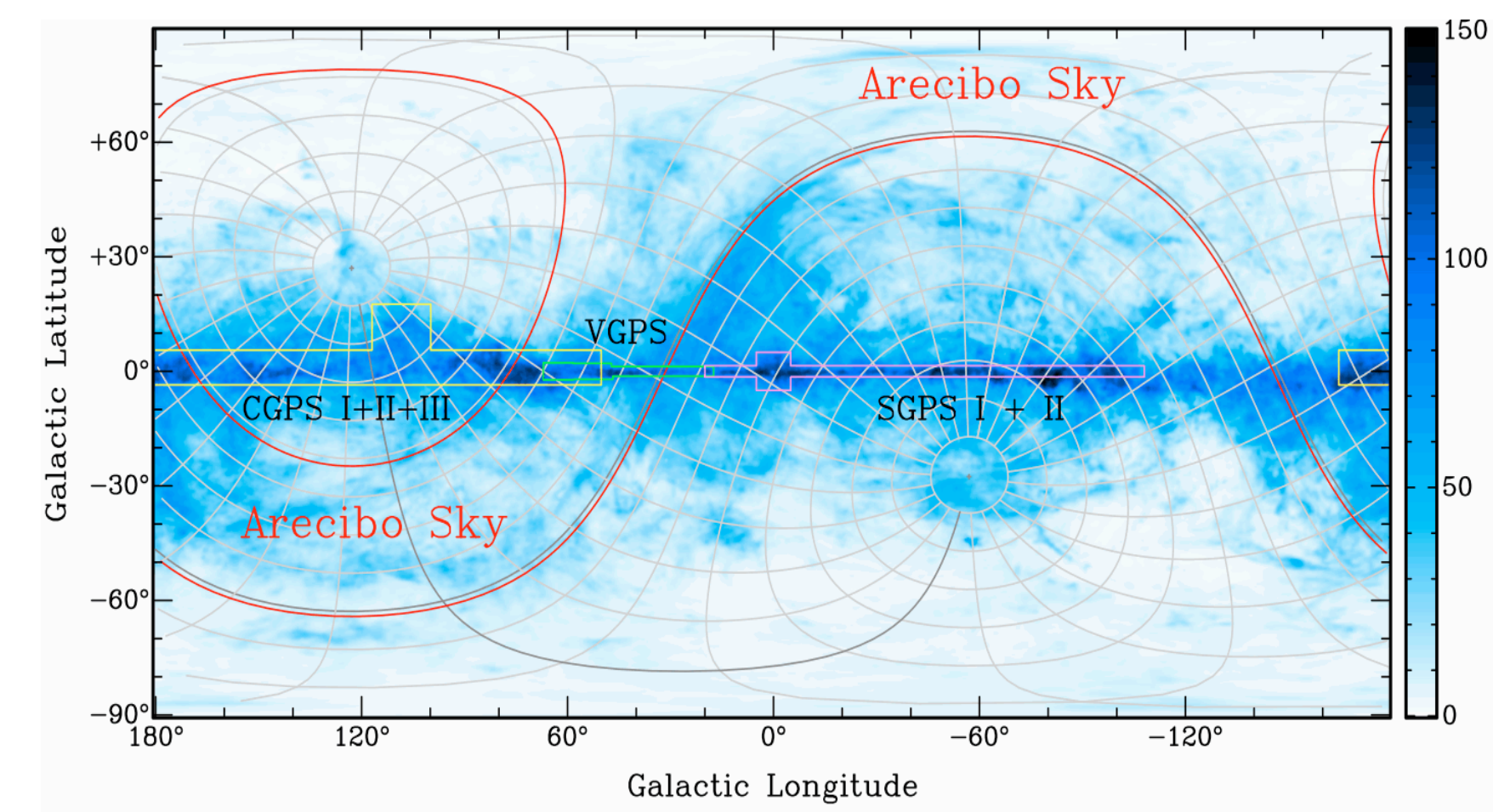


Figure 1. High-resolution 21cm H I and 2.6mm CO survey coverage on the sky (above; LAB H I image, Kalberla et al. 2005) and in the Galactic disk (above right; spiral arm model from Taylor & Cordes 1993). Arecibo is well suited to faint, high latitude emission studies, while the CGPS, VGPS, and SGPS are excellent for small-scale, low-latitude absorption. The grid is J2000 coordinates.

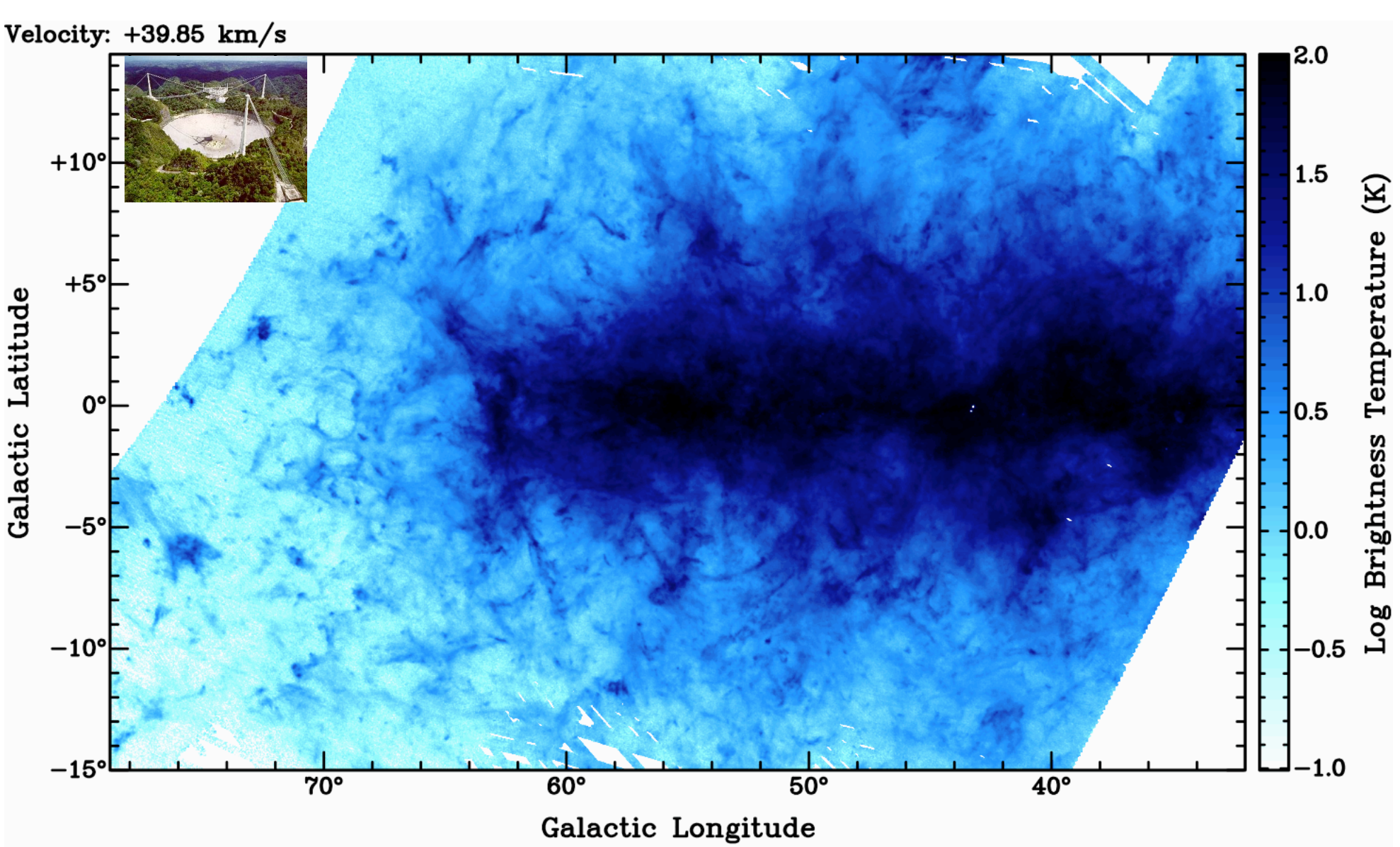


Figure 2. H I emission knots and filaments extending > 500 pc off the plane (I-GALFA 4' beam survey; Gibson et al. 2012). Many of these features are cold and may contain "dark" gas -- either opaque H I or CO-free H₂. Far-IR dust photometry is crucial for this investigation, just as H I and CO spectral line image cubes can greatly aid ISM dust studies.

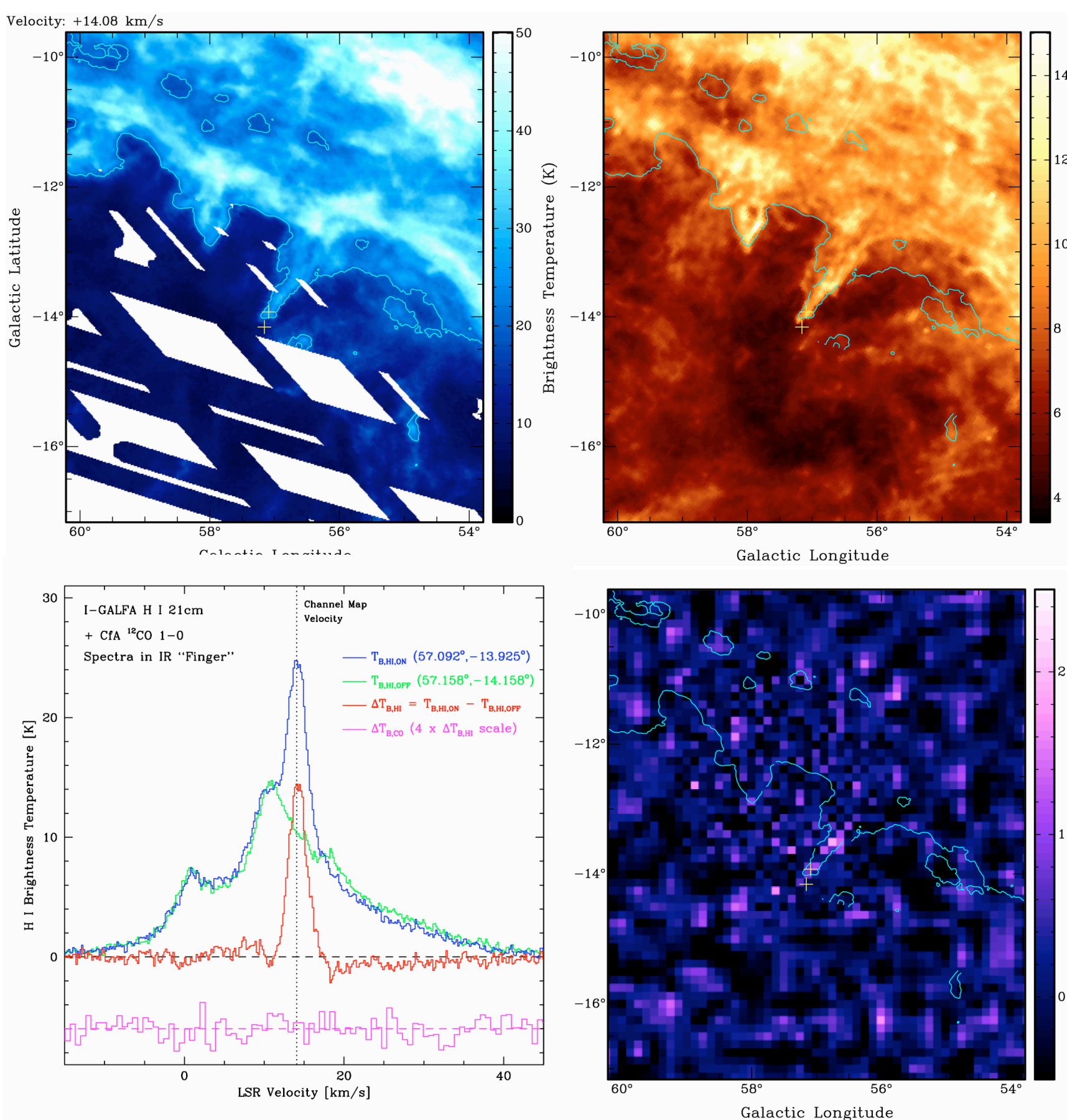


Figure 3. Prominent dark-gas filament in Arecibo narrow-line H I emission (NHIE; left panels) and IRIS 100 μ m dust (upper right; Miville-Deschenes & Lagache 2006), with little or no CfA ¹²CO 1-0 emission (lower right; Dame, private comm.); the contour is $T_B(\text{H I}) = 20$ K. $N_{\text{H I}}(\tau \ll 1) \sim 8 \times 10^{19} \text{ cm}^{-2}$, while multiplying the ON-OFF 100 μ m intensity by $1 \times 10^{20} \text{ cm}^{-2} / \text{MJy/sr}$ (Reach et al. 1994) yields $N_{\text{H I}}(\text{dust}) \sim 5 \times 10^{20} \text{ cm}^{-2}$, near the ¹²CO self-shielding limit but above that for dark H₂ (Snow & McCall 2006).

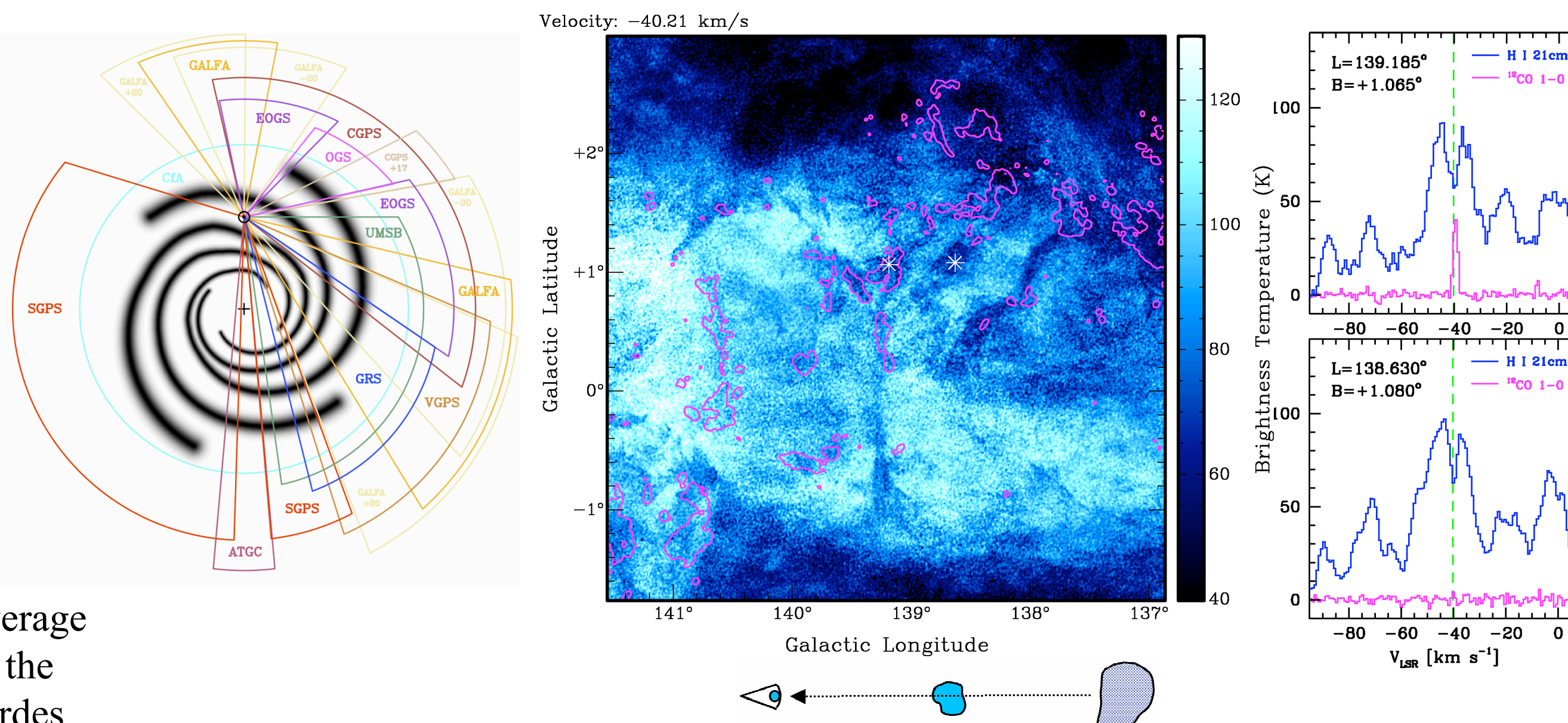
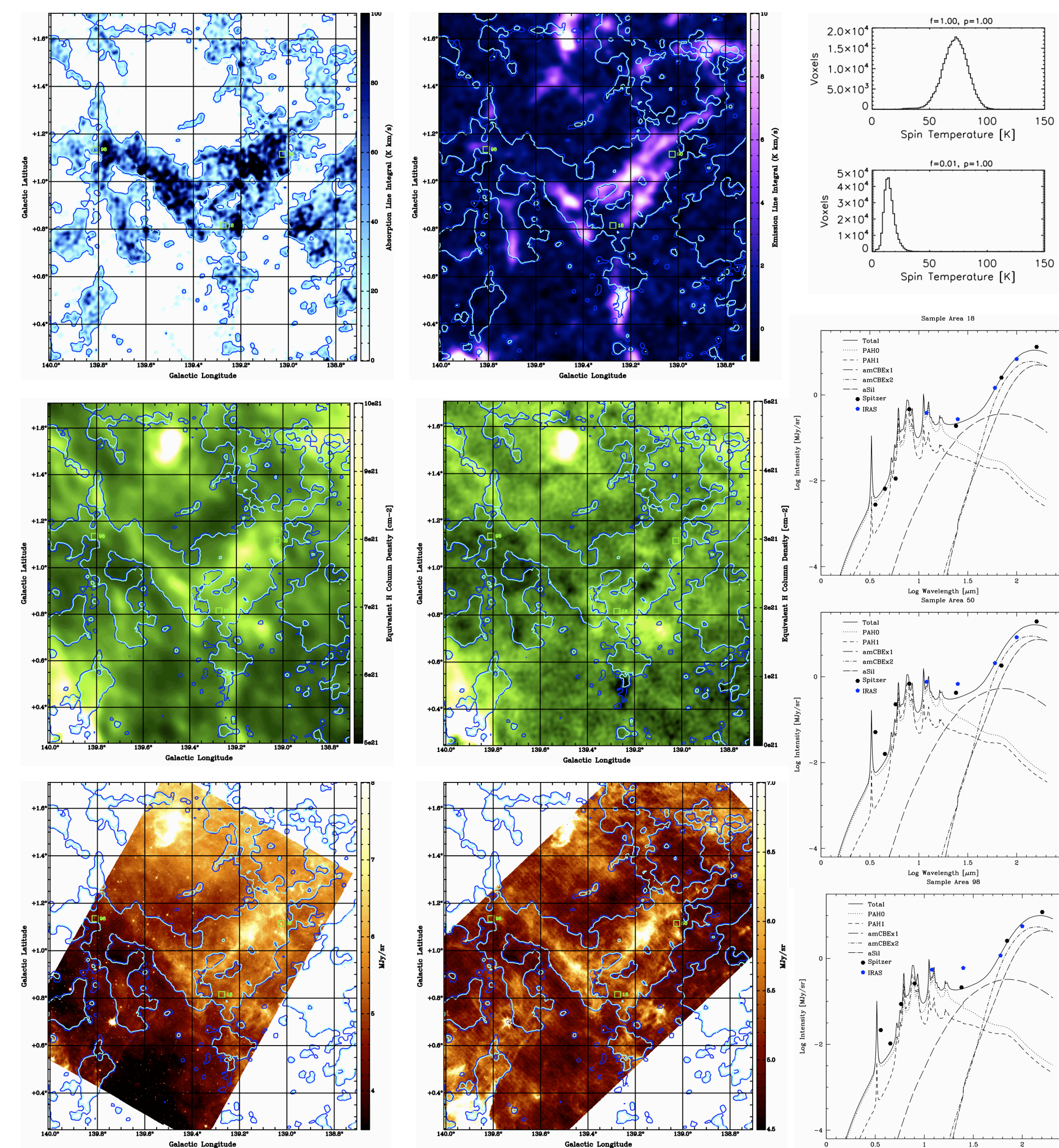


Figure 4. H I self-absorption (HISA) against warmer background H I emission (sketch) arises from atomic gas that is too cold to explain easily if it is not outside molecular clouds (Wolfire et al. 2003), and yet HISA shadows often appear separate from CO emission, particularly in the outer Galaxy. The panels above show 1' beam CGPS H I (blue; Taylor et al. 2003) and OGS ¹²CO 1-0 (magenta; Heyer et al. 1998). The clouds shown are ~ 2 kpc away in the Perseus arm, where they may be forming H₂ and CO downstream of the spiral shock before forming new stars (Gibson et al. 2005).

Figure 5. We have extracted HISA ON-OFF brightness difference maps (top left panel below; HISA contour in all maps) and have analyzed their properties using simple physical relationships (Gibson et al. 2000). We find temperatures like those of typical cold atomic or molecular gas, depending on the HISA partial pressure (top right). We also obtained $N_{\text{H I}}(\text{CO})$ from the line integral (top center) using an empirical factor $X_{\text{CO}} = 1.0 \times 10^{20} \text{ cm}^{-2} / (\text{K km/s})$ and $N_{\text{H I}}(\text{dust})$ from I_{100} (center left) as in Figure 3. When column densities of HISA, H I emission, and CO are all subtracted from the scaled dust column (center), residuals are near zero in the CO cloud cores, but significant IR excess appears in many areas, e.g., near $l, b = 139.9^\circ, +1.4^\circ$. We are pursuing more sophisticated SED fits of Spitzer data (bottom 8 + 24 μ m panels, right plots) with DustEM (Compiegne et al. 2011).



References

- Compiegne, M., et al. 2011, A&A, 525, 103
 Dame, T. M., et al. 2001, ApJ, 547, 792
 Gibson, S. J. 2010, ASPC, 438, 111
 Gibson, S. J., et al. 2012, AAS, 219, 349-29
 Gibson, S. J., et al. 2005, ApJ 626, 195
 Gibson, S. J., et al. 2000, ApJ, 540, 851
 Heyer, M. H., et al. 1998, ApJS, 115, 241
 Kalberla, P. M. W., et al. 2005, A&A, 440, 775
 Miville-Deschenes, M.-A., & Lagache, G. 2005, ApJS, 157, 302
 Reach, W. T., Koo, B.-C., & Heiles, C. 1994, ApJ, 429, 672
 Snow, T. W., & McCall, B. J. 2006, ARA&A, 44, 367
 Taylor, A. R., et al. 2003, AJ, 125, 3145
 Taylor J. H., & Cordes, J. M. 1993, ApJ, 411, 674
 Wolfire, M. G., et al. 2003, ApJ, 587, 278

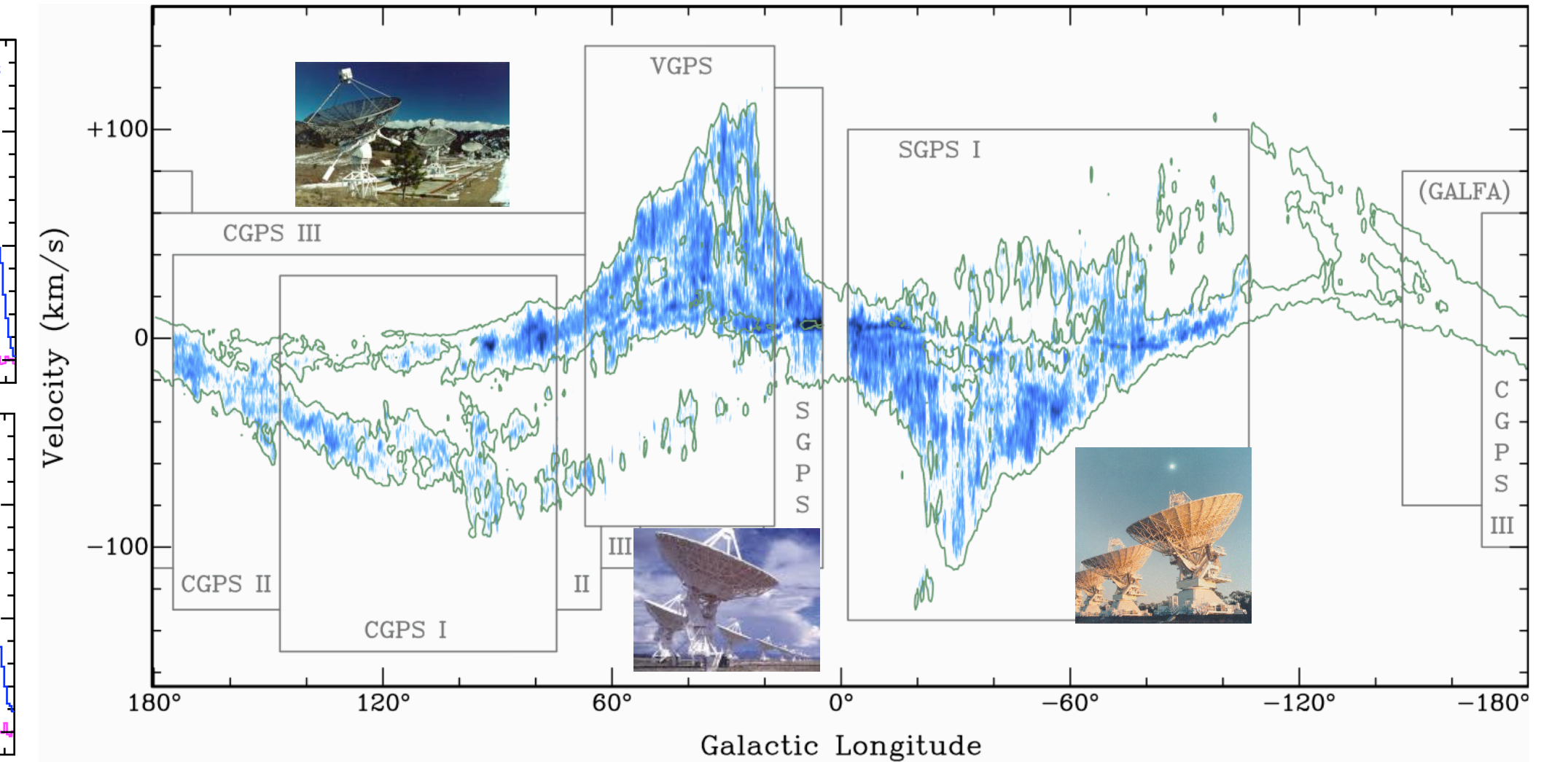
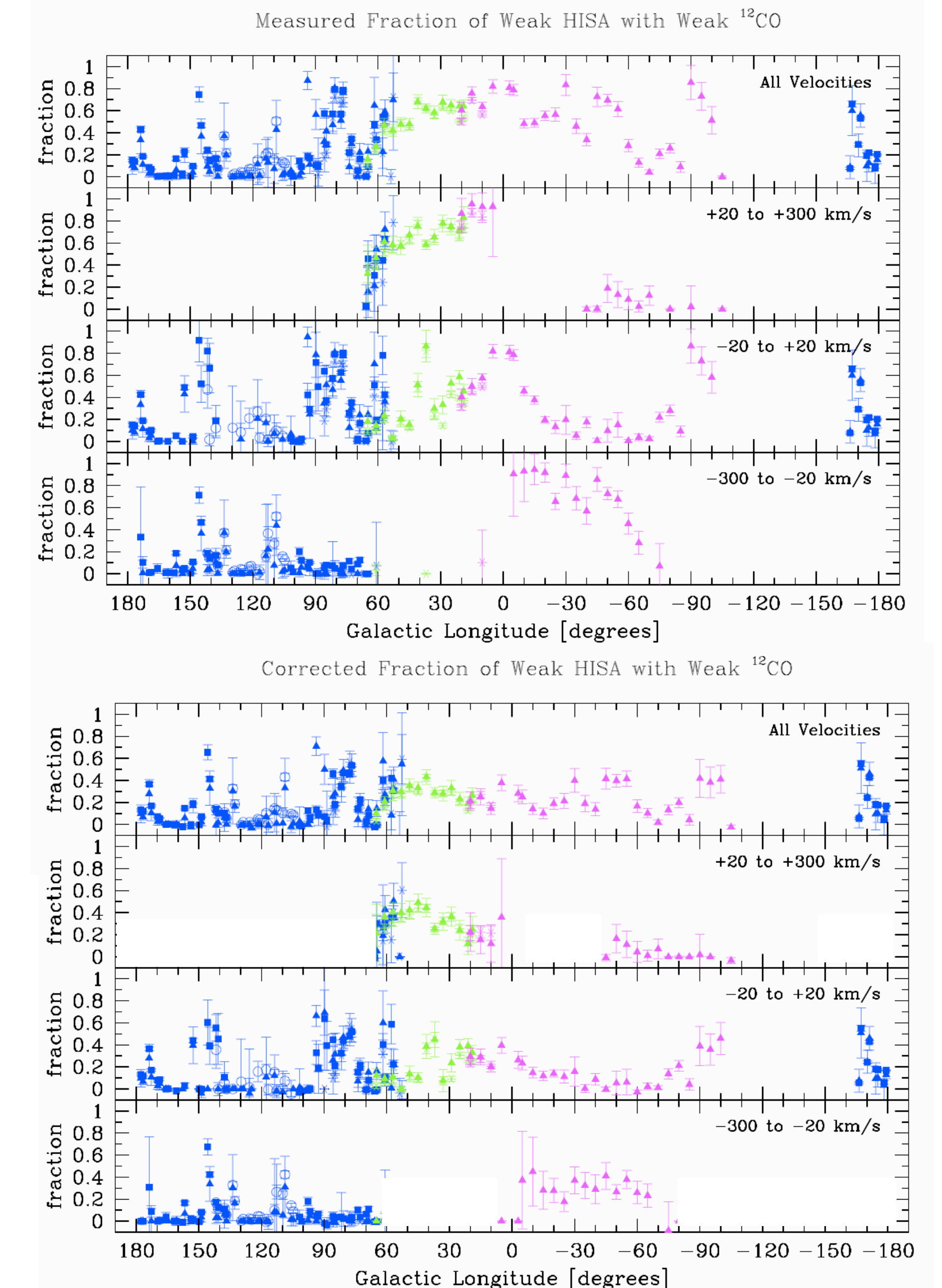


Figure 6. We have mapped HISA in the CGPS, VGPS, and SGPS, where it is widespread (top; Gibson 2010; green contour is search region). HISA traces spiral arms in the outer Galaxy and tangent points in the inner Galaxy, where arm structure is hard to distinguish (above). CfA CO (magenta; Dame et al. 2001) matches HISA poorly in the outer Galaxy and better in the inner Galaxy, as borne out by the fraction of HISA pixels containing CO vs. longitude (below). However, this is partly due to random alignments, which are more likely in the inner Galaxy where both CO and HISA are more abundant; subtracting such expected coincidences (bottom) leaves most HISA CO-free, "dark" gas.

Figure 6. We have mapped HISA in the CGPS, VGPS, and SGPS, where it is widespread (top; Gibson 2010; green contour is search region). HISA traces spiral arms in the outer Galaxy and tangent points in the inner Galaxy, where arm structure is hard to distinguish (above). CfA CO (magenta; Dame et al. 2001) matches HISA poorly in the outer Galaxy and better in the inner Galaxy, as borne out by the fraction of HISA pixels containing CO vs. longitude (below). However, this is partly due to random alignments, which are more likely in the inner Galaxy where both CO and HISA are more abundant; subtracting such expected coincidences (bottom) leaves most HISA CO-free, "dark" gas.



LEGEND	
CO Survey (SHAPES)	HISA Survey (COLORS)
Extended OGS (EOGS12)	Canadian Galactic Plane Survey (CGPS)
Outer Galaxy Survey (OGS)	VLA Galactic Plane Survey (VGPS)
Univ. of Mass-Stony Brook (UMSB)	Southern Galactic Plane Survey (SGPS)
Center for Astrophysics (CfA)	